J|A|C|S COMMUNICATIONS

Published on Web 01/19/2010

Nuclear Targeting of Gold Nanoparticles in Cancer Cells Induces DNA Damage, Causing Cytokinesis Arrest and Apoptosis

Bin Kang, Megan A. Mackey, and Mostafa A. El-Sayed*

Laser Dynamics Laboratory, School of Chemistry and Biochemistry, Georgia Institute of Technology, Atlanta, Georgia 30332-0400

Received December 4, 2009; E-mail: melsayed@gatech.edu

Understanding how nanomaterials affect live cell functions, controlling such effects, and using them for disease therapeutics are now the principal aims and most challenging aspects of nanobiotechnology and nanomedicine. Gold nanoparticles (AuNPs), nanorods, and nanoshells with unique properties[1−5] have been shown to be of potential use in anticancer drug delivery systems[6] and photothermal cancer treatment agents.[7−12] Although such applications have shown promising potential in cancer treatment, the fundamental interactions and effects of nanomaterials in living systems for the most part still remain unknown.

To address these fundamentals, many studies to assess the effect of introducing AuNPs into the cytoplasm of the cell have been done,[13−15] yet little is known about the effect of AuNPs at the nucleus of the cell. The cell nucleus functions to maintain all processes that occur within the cell, and any disruptions within the nucleus would subsequently affect the cell's DNA, thereby disturbing the highly regulated cell cycle.

Here we report the use of nuclear targeting of AuNPs to selectively disturb the division of cancer cells by the observation of cytokinesis arrest. Cytokinesis arrest was observed by AuNP dark-field imaging of live cells in real time,[16] which showed binucleate cell formation at late stages of mitosis, leading to the failure of complete cell division. Confocal microscopy and flow cytometry gave evidence that DNA damage and programmed cell death (apoptosis), respectively, accompany the observed cytokinesis arrest.

In order to selectively transport the AuNPs into the cancer cell nucleus, 30 nm AuNPs coated with polyethylene glycol (PEG) were bioconjugated with an arginine−glycine−aspartic acid peptide (RGD) and a nuclear localization signal (NLS) peptide. A detailed description of the experiment can be found in the Supporting Information (SI). RGD is known to target alpha v beta 6 integrins on the cell surface and enter the cytoplasm via receptor-mediated endocytosis.[17] NLS, which has a lysine−lysine−lysine−arginine−lysine (KKKRK) sequence, is known to associate with karyopherins (importins) in the cytoplasm, after which translocation to the nucleus occurs.[18] AuNPs conjugated with RGD only (RGD-AuNPs) exhibit cancer-cell-specific targeting, and AuNPs conjugated with RGD and NLS (RGD/NLS-AuNPs) exhibit cancer cell nucleus-specific targeting. In this study, human oral squamous cell carcinoma (HSC) having alpha v beta 6 integrins overexpressed on the cell surface[19] was used as the cancer cell model, and human keratinocytes (HaCat) were used as the normal cell model. The RGD-AuNPs specifically target the cytoplasm of cancer cells (Figure S2a in the SI) over that of normal cells (Figure S2c), and the RGD/NLS-AuNPs specifically target the nuclei of cancer cells (Figure S2b) over those of normal cells (Figure S2d).

To look at the effects of the specific nuclear localization of AuNPs in cancer cells, a full investigation of the cell cycle was carried out under various conditions. Cell-cycle arrest was determined by studying the full cell-cycle time and the dynamics of cell division in the presence of AuNPs by using long-term live-cell gold plasmonic scattering imaging on a homemade setup (see Figure S3). Figure 1 displays typical snapshots of the movies taken of cancer cell division (movies S1−S4 in the SI). In the absence of AuNPs (Figure 1A and movie S1), cancer cells begin the process of cytokinesis at 45 min (Figure 1A3). After complete cleavage furrow contraction, daughter cells were linked together by a cytoplasmic bridge, which was extended over time with the midbody at its center (Figure 1A6). Abscission occurred after 2 h, and the two daughter cells separated completely to form independent cells (Figure 1A7). A similar process was observed for cells incubated with 0.4 nM RGD-AuNPs (see Figure S4a and movie S2) and 0.1 nM RGD/NLS-AuNPs (see Figure S4b and movie S3), with the 0.1 nM RGD/NLS-AuNPs extending the full cell-cycle time by ∼4 h (Figure S5). However, for cells incubated with 0.4 nM RGD/NLS-AuNPs, complete cell division was not observed (Figure 1B; also see movie S4). The onset of cytokinesis proceeded with the same kinetics as in the untreated cells (Figure 1B1−4), but when the cleavage furrow was fully contracted, the cytoplasmic bridge did not extend (Figure 1B5,6); instead, the contractile ring relaxed, and the daughter cells fused back together to form a binucleate cell (Figure 1B7). Cytokinesis arrest was not observed in any normal cell groups here. This observation clearly demonstrates that a 0.4 nM concentration of AuNPs targeting the nucleus of cancer cells causes disruption of cytokinesis, thereby inhibiting these cells from completing cell division.

Within the present work, cytokinesis arrest was observed only in cancer cells treated with 0.4 nM RGD/NLS-AuNPs, suggesting that a disruption within the nucleus is the cause. To test this possibility, we investigated DNA double-strand breaks (DSBs) in cancer cells incubated with AuNPs. Figure 2 shows confocal images of cancer cells in which the cell nuclei are stained blue with DAPI and the DSB foci are seen as bright-green FITC fluorescence (see Methods in the SI). For untreated cells (Figure 2a) and cells with AuNPs present in the cytoplasm (Figure 2b), no DSBs were observed in the cell nuclei. However, for cells with 0.4 nM AuNPs present at the nucleus (Figure 2c), bright-green DSB foci were observed in the cell nuclei. DSBs can induce many different defects of cellular function and could be one reason for cell-cycle disruption, specifically cytokinesis arrest and subsequent apoptosis, as observed here. No DNA damage was observed in free-peptide-treated cancer cells.

The observations seen with imaging techniques occurred in only a few cases. In order to prove this phenomenon on a larger scale, flow cytometry was carried out on a large number of cells. Both cancer cells and normal cells were first synchronized at prometaphase with nocodazole and then released in fresh medium containing different concentrations of RGD-AuNPs and RGD/

10.1021/ja9102698

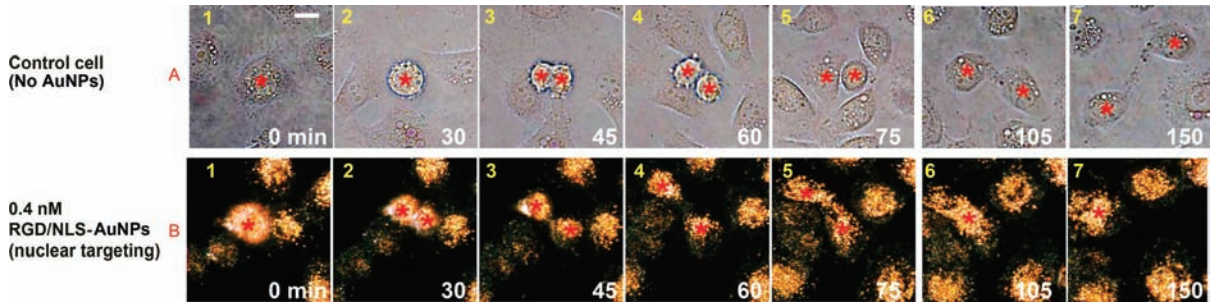

Figure 1. Real-time images of cancer cell division showing an apparent cytokinesis arrest (B4) followed by binucleate cell formation (B6, B7) in the presence of 0.4 nM nuclear-targeting gold nanoparticles (RGD/NLS-AuNPs) (also see movie S4 in the SI). This phenomenon was not observed in untreated cancer cells (A1−7) or cancer cells under other conditions (see Figure S3 and movies S2 and S3). Red stars indicate the nuclei. Scale bar: 10 μm.

NLS-AuNPs (see Methods in the SI). The flow cytometry results are shown in Figure 3 (for the original data, see Figure S6). In the absence of AuNPs, 90% of the cancer cell population was synchronized in the M phase at time zero (see the original data in Figure S6). At 120 min, more than 75% of the cell population had exited mitosis. Finally, at 360 min, more than 90% of the cell population was at the G1 phase. In the presence of 0.1 nM RGD/NLS-AuNPs, the process of cell division was slightly disrupted (slowed down), as indicated by the dynamics compared with the untreated cancer cells, but more than 80% of the cell population was able to go through mitosis and enter the G1 phase. In contrast, in the presence of 0.4 nM RGD/NLS-AuNPs, 60% of the cell population was at the M phase after 120 min, suggesting mitotic delay. At 360 min, 35% of the cell population was still arrested at the M phase, indicating that the cancer cells were unable to proceed through mitosis. As for the normal cells, all of the AuNP-treated groups showed no contrast to the untreated cells. Normal cells in all cases were able to proceed through mitosis.

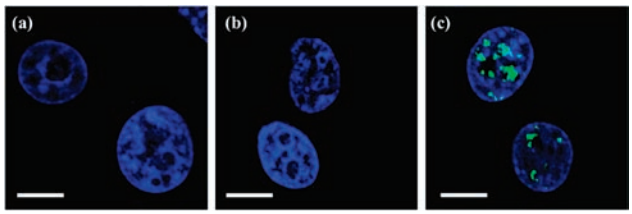

Figure 2. DNA damage induced by nuclear localization of gold nanoparticles in cancer cells in the presence of 0.4 nM nuclear-targeting gold nanoparticles (RGD/NLS-AuNPs) is indicated by the bright-green fluorescence in (c). Cancer cells (a) in the absence of AuNPs and (b) in the presence of a lower concentration of AuNPs showed no DNA damage. Scale bar: 10 μm.

As the last step of cell division, cytokinesis is very complex and highly regulated.[20] Errors in the cytokinesis process could potentially cause apoptosis. To further investigate the result of the observed cytokinesis arrest, a complete cell-cycle analysis via flow cytometry and subsequent identification of a subG1 cell population (apoptotic cells) was carried out (Figure 4).

Cancer cells and normal cells were grown in the presence of different concentrations of RGD-AuNPs and RGD/NLS-AuNPs for 24 h before being analyzed (see Methods in the SI). For cancer cells incubated with 0.4 nM RGD/NLS-AuNPs, ~20% of the cell population was apoptotic (yellow in Figure 4). This particular attribute was not observed in the untreated cancer cells, the other AuNP-treated cancer cells, or any of the normal cell cases (treated or untreated with AuNPs). In the normal cell group, cells treated with a 0.4 nM concentration of AuNPs showed accumulation of cells at the G1 phase, indicating a disruption of the G1-to-S transition in the cell cycle, but the AuNPs did not cause apoptosis, as indicated by the absence of a subG1 cell population (Figure S7). In control groups treated with free peptides, neither M-phase arrest nor G1 disruption were observed (Figure S8).

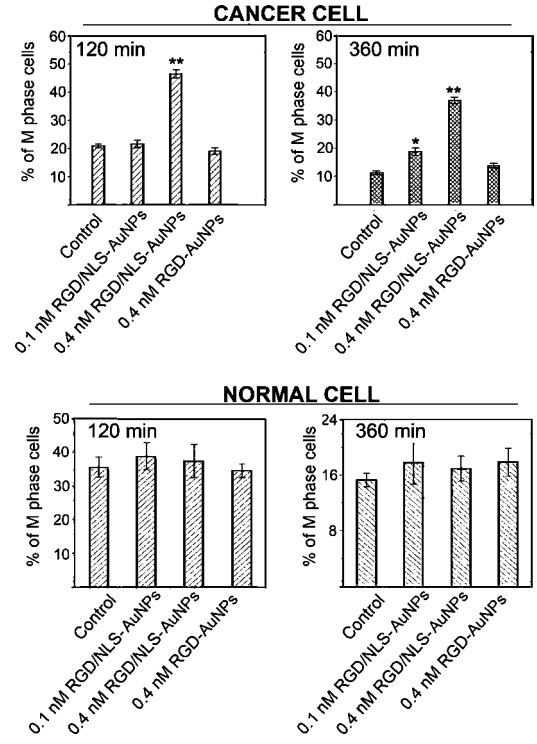

Figure 3. (top) M phase (mitosis phase of cell division) accumulation of cancer cells in the presence of 0.4 nM nuclear-targeting gold nanoparticles (RGD/NLS-AuNPs) suggests complete cell division (cytokinesis) has not taken place (see movie S4). (bottom) Data for normal cells. Nocodazole synchronization and release techniques were used in this experiment (see Methods in the SI; the original data are shown in Figure S6), and the cell cycle was measured at different times of release (120 and 360 min).

Upon observation of an apoptotic cell population, absolute cell numbers were counted under each condition (Figure S9). The cancer cell number did not significantly change with AuNPs present in the cytoplasm, but a significant decrease in the cell number (30%) was observed in the presence of 0.4 nM RGD/NLS-AuNPs. The normal cell number did not significantly change upon treatment with AuNPs. Here, both the subG1 cell population (20%) and cell number decrease (30%) were observed in only the cancer cells treated with 0.4 nM RGD/NLS-AuNPs.

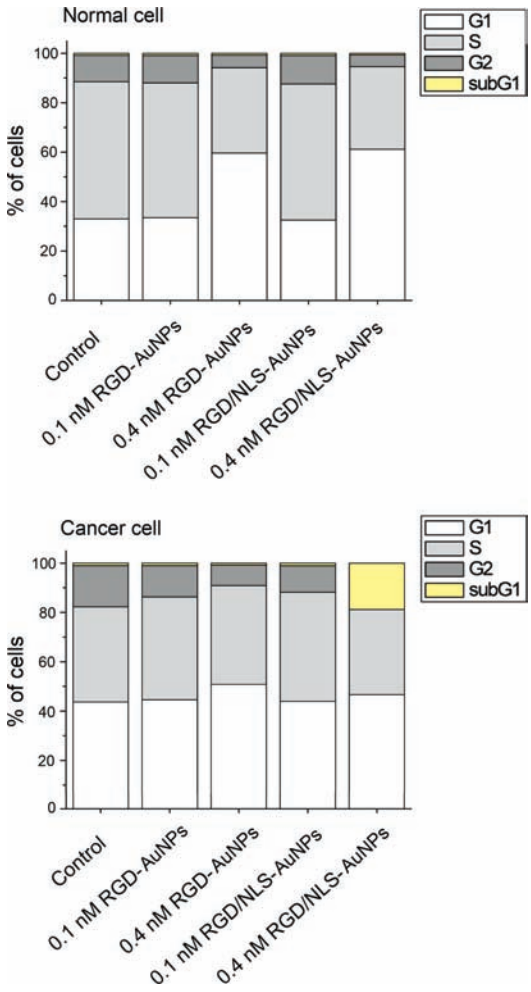

Figure 4. Percentages of cells in each phase of the cell cycle show the appearance of a DNA-deficient cell population (subG1, yellow) for cancer cells in the presence of 0.4 nM nuclear-targeting gold nanoparticles (RGD/NLS-AuNPs), suggesting apoptosis.

These results clearly show that the cytokinesis arrest observed in the live-cell imaging and synchronized cell flow cytometry for cancer cells in the presence of 0.4 nM RGD/NLS-AuNPs results in apoptosis.

In conclusion, we have demonstrated that nuclear targeting of gold nanoparticles in cancer cells cause cytokinesis arrest, leading to the failure of complete cell division and thereby resulting in apoptosis. This work shows evidence that nanomaterials localized at the cell nucleus can specifically affect cellular function. A detailed mechanism has not been established, yet the results shown here are still significant. These observations have implications in understanding the basic interactions between nanomaterials and live systems and have a huge impact on the fields of nanomedicine and nanobiology. These results might even propose a new method by which AuNPs can be used alone as an anticancer therapeutic material if conjugated to the proper nuclear-targeting ligands. The cytokinesis arrest observed here should be a general effect for other types of nanoparticles that can selectively target the nuclei of cancer cells.

Acknowledgment. We thank the Julius Brown Chair Funding (3306559GT) for financial support. B.K. thanks the China Scholar Council (2008683010) and Doctor Innovation Funds of NUAA (BCXJ08-09, China) for support. The authors thank Dr. W. Qian for help with the live-cell imaging setup, Dr. X. Huang for help with particle conjugation training, and Prof. A. K. Oyelere's group for providing some initial peptide samples.

Supporting Information Available: Detailed experimental methods, live-cell imaging setup, original data from the cell-cycle analyses, and supporting movies (AVI). This material is available free of charge via the Internet at http://pubs.acs.org.

References

(1) El-Sayed, M. A. *Acc. Chem. Res.* **2001**, *34*, 257–264.
(2) Burda, C.; Chen, X. B.; Narayanan, R.; El-Sayed, M. A. *Chem. Rev.* **2005**, *105*, 1025–1102.
(3) Link, S.; El-Sayed, M. A. *Int. Rev. Phys. Chem.* **2000**, *19*, 409–453.
(4) Boisselier, E.; Astruc, D. *Chem. Soc. Rev.* **2009**, *38*, 1759–1782.
(5) Daniel, M. C.; Astruc, D. *Chem. Rev.* **2004**, *104*, 293–346.
(6) Paciotti, G. F.; Myer, L.; Weinreich, D.; Goia, D.; Pavel, N.; McLaughlin, R. E.; Tamarkin, L. *Drug Delivery* **2004**, *11*, 169–183.
(7) Hirsch, L. R.; Stafford, R. J.; Bankson, J. A.; Sershen, S. R.; Rivera, B.; Price, R. E.; Hazle, J. D.; Halas, N. J.; West, J. L. *Proc. Natl. Acad. Sci. U.S.A.* **2003**, *100*, 13549–13554.
(8) O'Neal, D. P.; Hirsch, L. R.; Halas, N. J.; Payne, J. D.; West, J. L. *Cancer Lett.* **2004**, *209*, 171–176.
(9) Loo, C.; Lowery, A.; Halas, N.; West, J.; Drezek, R. *Nano Lett.* **2005**, *5*, 709–711.
(10) Huang, X. H.; El-Sayed, I. H.; Qian, W.; El-Sayed, M. A. *J. Am. Chem. Soc.* **2006**, *128*, 2115–2120.
(11) El-Sayed, I. H.; Huang, X. H.; El-Sayed, M. A. *Cancer Lett.* **2006**, *239*, 129–135.
(12) Dickerson, E. B.; Dreaden, E. C.; Huang, X. H.; El-Sayed, I. H.; Chu, H. H.; Pushpanketh, S.; McDonald, J. F.; El-Sayed, M. A. *Cancer Lett.* **2008**, *269*, 57–66.
(13) Chithrani, B. D.; Chan, W. C. W. *Nano Lett.* **2007**, *7*, 1542–1550.
(14) Chithrani, B. D.; Ghazani, A. A.; Chan, W. C. W. *Nano Lett.* **2006**, *6*, 662–668.
(15) Jiang, W.; Kim, B. Y. S.; Rutka, J. T.; Chan, W. C. W. *Nat. Nanotechnol.* **2003**, *3*, 145–150.
(16) Qian, W.; Kang, B.; Huang X. H.; El-Sayed, M. A. *J. Biomed. Opt.*, submitted.
(17) Gao, H. J.; Shi, W. D.; Freund, L. B. *Proc. Natl. Acad. Sci. U.S.A.* **2005**, *102*, 9469–9474.
(18) Nakielny, S.; Dreyfuss, G. *Cell* **1999**, *99*, 677–690.
(19) Xue, H.; Atakilit, A.; Zhu, W. M.; Li, X. W.; Ramos, D. M.; Pytela, R. *Biochem. Biophys. Res. Commun.* **2001**, *288*, 610–618.
(20) Scholey, J. M.; Brust-Mascher, I.; Mogilner, A. *Nature* **2003**, *422*, 746–752.

JA9102698